AN EXTENDED SPS LONGITUDINAL IMPEDANCE MODEL

José E. Varela, T. Argyropoulos, T. Bohl, F. Caspers, J. F. Esteban Müller, J. Ghini, A. Lasheen, D. Quartullo, B. Salvant, E. Shaposhnikova, C. Zannini, CERN, Geneva, Switzerland

Abstract

Longitudinal multi-bunch instability in the CERN SPS with a very low intensity threshold is a serious limitation for the future doubling of bunch intensity required by the HL-LHC project. A complete and accurate impedance model is essential to understand the nature of this instability and to plan possible cures. This contribution describes the current longitudinal impedance model of the SPS. Electromagnetic simulations and bench measurements were used to build the model. The contribution from each element is described and compared to the total machine impedance. Together with relevant beam measurements and simulations, the analysis of the different sources of impedance is used to identify the source of the longitudinal instability limiting the SPS performance so that the responsible elements can be acted upon.

INTRODUCTION

At the end of the LHC Run 1 in 2012 the beam with 25 ns bunch spacing and with an intensity of 1.3×10^{11} p/b was successfully accelerated in the SPS. However, for the intensity of HL-LHC ($\sim 2.5 \times 10^{11}$), the SPS bunches will be too long for the LHC capture with the existing 400 MHz RF system. This limitation comes from beam loading and longitudinal beam instabilities in the SPS. As a part of the LHC Injectors Upgrade (LIU) project [1], instabilities were studied by means of beam measurements and simulations [2,3]. The simulations rely on having an accurate impedance model of the machine. This paper describes the current status of the SPS longitudinal impedance model which was recently updated with the contribution from the vacuum flanges [4]. This model is then used in macroparticle simulations and the results are compared to beam measurements.

LONGITUDINAL IMPEDANCE MODEL

The longitudinal impedance model of the SPS currently accounts for the accelerating and Landau cavities, the extraction kickers, the vacuum flanges, the Beam Position Monitors (BPM), the pumping ports, the so-called Y-chambers, the beam scrapers and resistive wall as well as space charge impedance at low energy. The main contributors are the accelerating cavities, the extraction kickers and the vacuum flanges. Recently, the focus has been put on the accurate characterization of the Higher Order Modes (HOM) of the RF cavities and on the electrostatic and magnetic septa.

Cavities

The SPS has two RF systems, four 200 MHz Traveling Wave Cavities (TWC) and two 800 MHz TWC. The existing impedance model for the fundamental pass-band of the cavities is [5]

$$Z(\omega) = R\left[\left(\frac{\sin(\tau/2)}{\tau/2}\right)^2 - 2j\frac{\tau - \sin(\tau)}{\tau^2}\right], \qquad (1)$$

with $\tau = (\omega - \omega_0)l/v_g(\omega)$, where l is the length of the cavity, $v_g(\omega)$ is the frequency dependent group velocity and R the impedance at the center frequency ω_0. This model assumes perfect main coupler matching to the traveling wave inside the cavity. It has to be highlighted that the dependence on frequency of the group velocity is specially important for the 200 MHz cavities, as it introduces a significant asymmetry in the impedance spectrum.

There are two $\sim$ 16 m and $\sim$ 20 m long 200 MHz cavities. They have $R = 875$ kΩ and $R = 1.4$ MΩ, respectively. The 800 MHz cavities are $\sim$ 3 m long and are modeled with $R = 970$ kΩ. Finally, there is one known longitudinal HOM in the 200 MHz cavities at 629 MHz. With the existing HOM damping, this HOM can be described as a resonator with $R = 108$ and 86 kΩ and $R/Q = 430$ and 346 Ω for the long and short cavities, respectively.

The black lines in Fig. 1 show the modulus of the total longitudinal impedance of the SPS in both linear and logarithmic scales. The two biggest peaks, at 200 and 800 MHz, are the contributions from the fundamental pass-bands of the cavities.

Kickers

The SPS kickers are the biggest source of longitudinal broadband impedance. A fast extraction kicker system was

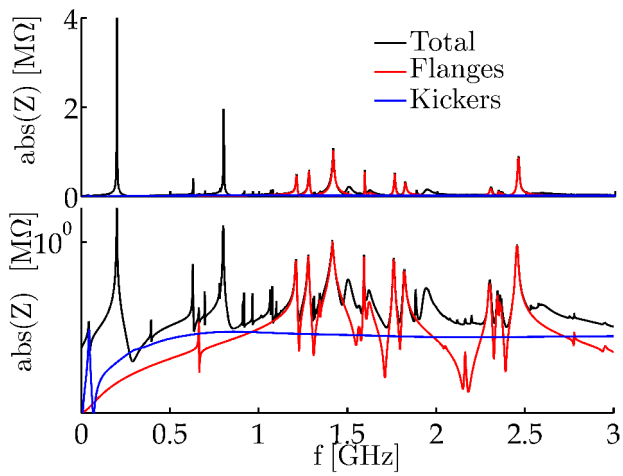

Figure 1: Modulus of the current longitudinal impedance of the SPS. The red and blue traces show the contribution of the vacuum flanges and the kickers, respectively. The top and bottom plots show the impedance in linear and logarithmic scale, respectively.

ISBN 978-3-95450-168-7

installed in the SPS in 2003 to meet the LHC specifications. Since the beam induced heating of these devices was observed to be critical, each kicker was equipped with a cooling system. The beam induced heating is directly related to the beam power loss through the real part of the longitudinal impedance. Various impedance reduction techniques were investigated in order to minimize the beam induced heating. Finally, the usage of silver fingers printed by serigraphy directly on the ferrite was implemented in 2007 [6]. Now, all eight extraction kickers are serigraphed.

The relative contribution of the extraction kickers [7] to the total longitudinal impedance in the SPS can be checked in Fig. 1. The logarithmic scale plot shows that these elements give a ~ 20 kΩ offset starting from ~ 500 MHz. Finally, there is the 44 MHz resonance produced by the serigraphed fingers which was studied in detail in [7].

Vacuum Flanges

The vacuum flanges are the biggest source of resonant impedance in the SPS. These elements have been object of study for the last two years. Due to the high number of different vacuum chambers, there are many types of interconnects. Vacuum flanges have been classified in two groups (according to connecting beam pipes) containing approximately 400 and 240 flanges, respectively [4]. The longitudinal impedance has been carefully evaluated for each type by means of both, full-wave simulations and RF measurements.

These elements are, most importantly, responsible for two high-impedance resonances at 1.4 and 2.3 GHz. The 2.3 GHz resonance has a relatively low R/Q and a high-Q. The 1.4 GHz resonance has a low Q, but a high R/Q. Once more, Fig. 1 can be used to compare the relative contribution of the vacuum flanges to the total impedance model. Figure 1 shows that these elements also contribute with non-negligible resonances at 1.2, 1.3, 1.6, 1.8 and 1.9 GHz.

Electrostatic and Magnetic Septa

Recently, the longitudinal impedance of the electrostatic (ZS) and magnetic septa (MS) was studied in more detail. These structures are remarkably complex and a high number of details need to be carefully accounted for. Both structures contain different very thin elements, for instance the wire array of the ZS or the isolating sheets of the MS. In addition, the different high-voltage ports play an important role in the overall impedance of the structure and are not easy to model.

These septa are placed in relatively big vacuum tanks (346 and 300 mm radius and 2.5 and 3.2 m long for the MS and ZS, respectively). This gives rise to a number potentially dangerous low frequency resonances. Figure 2 shows the real and imaginary parts of the longitudinal impedance of 25 MS and 5 ZS compared to the longitudinal impedance of the kickers. Usually, the impedance of the kickers is used as a reference to assess the importance of the impedance contribution of other elements in the SPS. Figure 2 shows, below ~ 500 MHz, some resonances well above the kicker impedance. Preliminary measurements suggest that simulations underestimate the losses in these structures. Therefore,

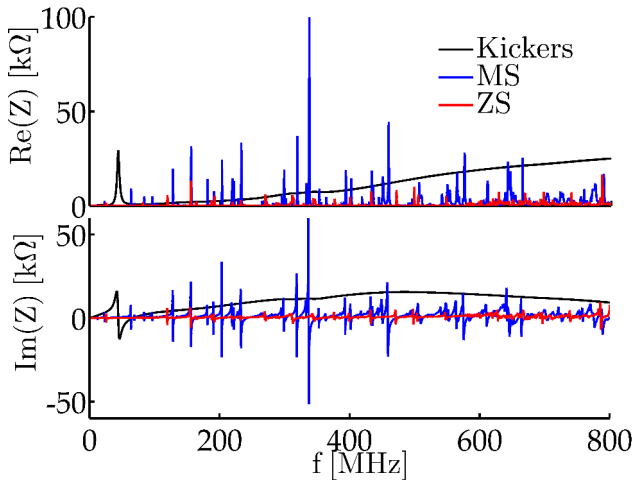

Figure 2: Real and imaginary parts of the longitudinal impedance of 25 MS and 5 ZS compared to the total longitudinal kicker impedance.

the impedance of these elements should be smaller than the one presented in Fig. 2. Due to this uncertainty, the impedance of the ZS and MS has not yet been included in the SPS impedance model.

Other Contributions

The SPS longitudinal impedance model also includes around 200 BPMs. There are two main types of BPMs, the horizontal (BPH) and the vertical (BPV) monitors. The around hundred BPHs in the SPS have two significant resonances, at 1.6 and 1.9 GHz. These two resonances have an R/Q around 1 kΩ and a longitudinal impedance of 100 kΩ.

In addition, the current impedance model also includes the contributions from other sources like shielded and unshielded pumping ports, Y-chambers and the beam scrapers. The limited number of these elements makes their relative contribution small compared to the total SPS impedance. Finally, the resistive wall impedance was analytically estimated accounting for the different vacuum chambers in the SPS [7].

BEAM MEASUREMENTS AND SIMULATIONS

Beam measurements and macroparticle simulations using the described SPS impedance model were carried out in order to understand the nature of the longitudinal instability observed in the SPS and to identify the responsible impedance sources. In operation, these instabilities are cured by using the 800 MHz RF system and controlled longitudinal emittance blow up.

Above some intensity threshold, uncontrolled longitudinal emittance blow-up is observed during the acceleration ramp for both single and multi-bunch LHC beams. An example for single bunches in a double RF system (bunch shortening mode) is shown in Fig. 3, where measured and simulated bunch lengths at the SPS flat top are plotted together. The

ISBN 978-3-95450-168-7

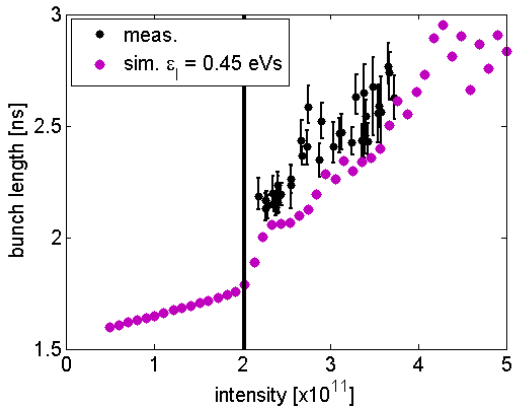

Figure 3: Measured and simulated bunch length as a function of intensity for a single bunch at the SPS flat top in a double RF system (bunch shortening mode). The voltage at 200 MHz was 2 MV and at 800 MHz 200 kV.

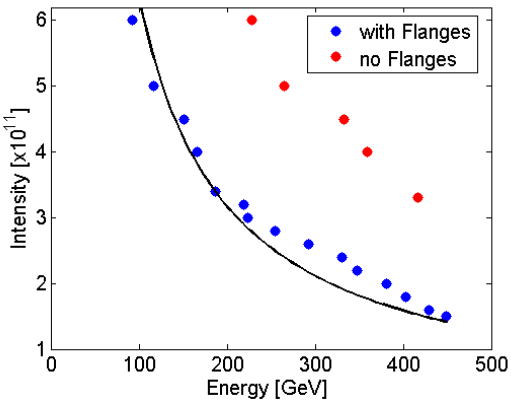

Figure 4: Single-bunch instability threshold through the ramp from macroparticle simulations using the longitudinal impedance model with (blue dots) and without (red dots) vacuum flanges. The 200 MHz voltage was calculated for a constant bucket area of 0.5 eVs and kept at 2 MV at the end of the ramp and flat top. Intensity threshold scaling $\sim 1/E$ is shown as a line.

results are in good agreement with a strong increase of the bunch length with intensity observed above $\sim 2 \times 10^{11}$ p/b. This increase can not be attributed to the potential well distortion. Thus, microwave instability due to some high frequency resonant impedance could be responsible for this effect.

Indeed, measurements with very long bunches ($\sim$ 25 ns) and RF off at the SPS flat bottom revealed a strong peak at $\sim$ 1.4 GHz [8]. The impedance of vacuum flanges with a strong resonant peak at 1.4 GHz (among others) can be responsible for this uncontrolled emittance blow-up.

The latter is also confirmed by macroparticle simulations using the SPS longitudinal impedance model. In Fig. 4 the single-bunch instability thresholds found through the ramp for different beam intensities are shown. At all beam energies, without the impedance of the vacuum flanges (red dots) the intensity thresholds are practically twice as high. All bunches in simulations had 2.7 ns bunch length at flat bottom.

In addition, the quality factor Q $\approx$ 200 of the 1.4 GHz resonance of the vacuum flanges is consistent with the experimental observation that only a few bunches spaced by 25 ns or 50 ns are coupled during the instability, but the distance of 225 ns between the batches is enough to practically fully decouple them (instability thresholds in the SPS with 1 or 4 batches are very similar). That is why no coupled-bunch mode could be identified. This is also confirmed by ongoing macroparticle simulations for 12 bunches spaced by 25 ns.

CONCLUSIONS

The current longitudinal impedance model for the SPS is presented. The most relevant contributors are the accelerating cavities, the broadband impedance of the extraction kickers and the high-frequency resonances of the vacuum flanges. Using the described longitudinal impedance model, beam dynamics simulations show good agreement with beam measurements. The single-bunch instability threshold was found to be more than two times higher without the contribution of the vacuum flanges. Therefore, these elements are, at least, responsible for the single-bunch instability in the SPS. Among other potential solutions, an impedance reduction campaign to minimize the impedance of the vacuum flanges during the Long Shutdown 2 (2019) is under discussion.

REFERENCES

[1] "LHC Injectors Upgrade Technical Design Report" edited by J. Coupard *et al.*, CERN-ACC-2014-0337.

[2] E. Shaposhnikova *et al.*, "Identifiaction of High-Frequency Resonant Impedance in the CERN SPS," Proc. of IPAC2014, p. 1416-1418 (2014).

[3] T. Argyropoulos, E. Shaposhnikova and J. E. Varela, "Other Means to Increase the SPS 25 ns Performance - Longitudinal Plane," Proc. LHC Performance Workshop, Chamonix, France (2014).

[4] J. E. Varela, "Longitudinal Impedance Characterization of the CERN SPS Vacuum Flanges," IPAC 15, these Proc.

[5] G. Dôme, "The SPS Acceleration System Travelling Wave Drift-Tube Structure for the CERN SPS," Internal Note SPS/ARF/77-11 (1977).

[6] T. Kroyer, F. Caspers and E. Gaxiola, "Longitudinal and Transverse Wire Measurements for the Evaluation of Impedance Reduction Measures on the MKE Extraction Kickers," Internal Note, AB-Note-2007-028 (2007).

[7] C. Zannini, "Electromagnetic simulations of CERN accelerator components and experimental applications," PhD thesis, Lausanne, EPFL, CERN-THESIS-2013-076 (2013).

[8] T. Argyropoulos *et al.*, "Identification of the SPS Impedance at 1.4 GHz," Proc. IPAC'13, Shanghai, China (2013).